MPC-Based Process Control of Deep Drawing: An Industry 4.0 Case Study in Automotive

Graziana Cavone, *Member, IEEE*, Augusto Bozza, *Graduate Student Member, IEEE*, Raffaele Carli, *Senior Member, IEEE*, and Mariagrazia Dotoli, *Senior Member, IEEE*

***Abstract*— Deep drawing is a metalworking procedure aimed at getting a cold metal sheet plastically deformed in accordance with a pre-defined mould. Although this procedure is well-established in industry, it is still susceptible to several issues affecting the quality of the stamped metal products. In order to reduce defects of workpieces, process control approaches can be performed. Typically, process control employs simple proportional-integral-derivative (PID) regulators that steer the blank holder force (BHF) based on the error on the punch force. However, a single PID can only control single-input single-output systems and cannot handle constraints on the process variables. Differently from the state of the art, in this paper we propose a process control architecture based on Model Predictive Control (MPC), which considers a multi-variable system model. In particular, we represent the deep drawing process with a single-input multiple-output Hammerstein-Wiener model that relates the BHF with the draw-in of *n* different critical points around the die. This allows the avoidance of workpiece defects that are due to the abnormal sliding of the metal sheet during the forming phase. The effectiveness of the proposed process controller is shown on a real case study in a digital twin framework, where the performance achieved by the MPC-based system is analyzed in detail and compared against the results obtained through an ad-hoc defined multiple PID-based control architecture.**

***Note to Practitioners*—This work is motivated by the emerging need for the effective implementation of the zero-defect manufacturing paradigm in the Industry 4.0 framework. Especially in the deep drawing process, various quality issues in stamped parts can lead to significant product waste and manufacturing inefficiencies. This turns into considerable economic losses for companies, particularly in the automotive sector, where deep drawing is one of the most used cold sheet metal forming techniques. In most applications, only sample inspections are performed on batches of finished-product, with subsequent losses of time and resources. For the sake of improving the workpiece quality, innovative strategies for real-time process control represent a viable and promising solution. In this context, the proposed MPC-based process control approach allows the correct shaping of the metal sheet that is getting deformed during the forming stroke, thanks to the draw-in monitoring at various locations around the die. The draw-in is indeed one of the most effective forming variables to control in order to provide a correct BHF during the forming stroke. A useful and easy-to-implement nonlinear metal sheet deep drawing process model is provided by this paper to perform an innovative process control strategy. A comprehensive methodology is applied in detail to an automotive case study, ranging from process modeling (model identification and validation based on experimental data acquisition) to MPC implementation (controller tuning and testing and software-in-the-loop system validation). The presented method can be easily implemented on any real deep drawing press, providing the multivariable constrained process with a suitable control system able to make the stamped parts well formed.**

***Index Terms*— Metal deep drawing process control, zero-defect manufacturing, real-time process control, model predictive control, software-in-the-loop simulation.**

Manuscript received 28 January 2022; accepted 24 March 2022. Date of publication 30 May 2022; date of current version 5 July 2022. This article was recommended for publication by Associate Editor L. Moench and Editor A. Cheng upon evaluation of the reviewers' comments. This work was supported in part by the Italian University and Research Ministry through the project Pico&Pro (National Research Program) under Contract ARS01_01061 and the project Maia (National Research Program) under Contract ARS01 00353 and in part by the National Natural Science Foundation of China under Grant 61950410604. *(Corresponding author: Graziana Cavone.)*

The authors are with the Department of Electrical and Information Engineering, Polytechnic of Bari, 70125 Bari, Italy (e-mail: graziana.cavone@poliba.it; augusto.bozza@poliba.it; raffaele.carli@poliba.it; mariagrazia.dotoli@poliba.it).

Color versions of one or more figures in this article are available at https://doi.org/10.1109/TASE.2022.3177362.

Digital Object Identifier 10.1109/TASE.2022.3177362

I. Introduction

DEEP drawing is a metalworking process used to impress a predefined shape to a metal sheet. The deformation of the metal is performed at re-crystallization temperature, which is usually equal to the ambient one for many metals [1]. In such a type of forming process, the metal sheet gets deformed plastically while it is pushed down into the die cavity, conforming it to its shape [1], and with no alterations in its thickness [2]. A schematic representation of a typical stamping press used for cold sheet metal forming is shown in Fig. 1. It consists of a *punch* (or *upper die*), a *die*, and a *blank holder*, which holds the metal sheet in place during the punch stroke (i.e., while the punch is lowered into the die). The blankholder design can also include appropriate *drawbeads* to help regulate the material flow into the die. Deep drawing is typically characterized by high pressures (generally, the magnitude is around 10 kPa), high speeds (up to 8 mm/s), and very short durations (less than 5 s). This results in high production rates, low labour costs, but difficulties in effectively controlling in real time the process [3]–[5].

Several quality issues affect the stamped metal products: the most common problems include *wrinkling* (due to compression stresses), *tearing* (due to tensile stresses), and *springback* (due to elasticity) [6], as illustrated in Fig. 2. During the forming phase, the occurrence of the listed defects can be identified by monitoring specific forming variables, i.e., the punch force, wrinkle height, draw-in, and friction force, which are all influenced by the blank holder force (BHF). In effect,

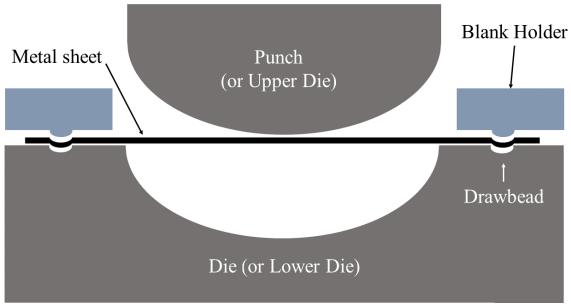

Fig. 1. Schematic representation of a typical stamping press configuration.

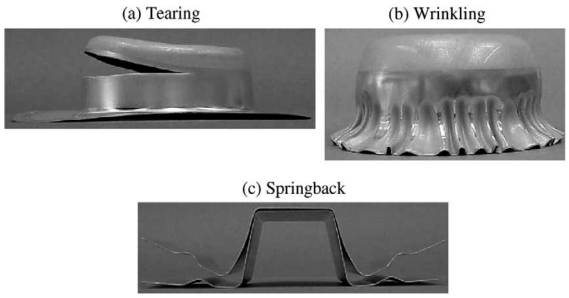

Fig. 2. The most common problems in the cold metal sheet forming [6].

the workpiece quality depends on how much the BHF presses on the blank holder: if it is too high, then the flow of material into the die is restricted and tearing is likely to occur in that region; if the BHF is too low, then excessive material flow can lead to wrinkling. Moreover, the BHF plays a crucial role in controlling springback, since it can change the internal force and metal flow resistance of a plate [7]. In fact, springback is due to deformations of the material in the elastic-plastic field. This is a critical aspect of the drawing process, especially in the automotive sector, where high accuracy is often required [2].

Due to the presence of the above described issues, the industrial deep drawing process is lagging behind in the full implementation of the zero-defect manufacturing (ZDM) paradigm. In fact, traditional methods used to pragmatically enhance the products quality typically consist in batch checking the stamped parts features. In case of defects in the examined part, the entire batch is backward checked, with consequent loss of time and a high number of defective parts. More recent and innovative approaches in Industry 4.0 consider the application of automatic control techniques [8], [9], which can be classified into *machine control* and *process control* [10], [11]. The first class of techniques aims at monitoring and controlling the press variables (e.g., feedback and control of the BHF, imposing the tracking of a predetermined trajectory), resulting in an open-loop control with respect to the process features, whereas the latter class aims at monitoring the forming parameters of the process and controlling the machine variables (e.g., feedback of the punch stroke and control of the BHF), thus resulting in a closed-loop control of the process parameters. Differently from machine control, process control can allow to online monitor the state of the stamped

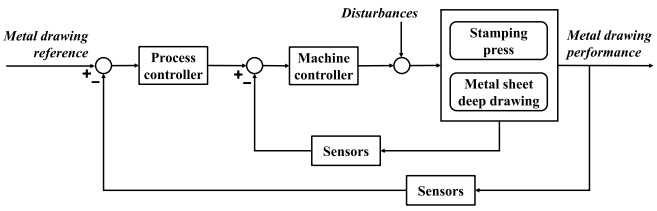

Fig. 3. Block diagram of a typical process control closed-loop.

part during the formation phase and to provide corrective actions in case of abnormal behaviors of the metal sheet, thus ensuring a more precise and higher quality control of the process [10]. As depicted in Fig. 3, machine and process control can be combined. Thus, the machine control feedback loop can be nested inside the process control one. In this manner, the process controller performs as a high-level control and provides a very important contribution to disturbance rejection.

In this context, the goal of this paper is twofold. On the one hand, we aim at contributing to the definition of a proper dynamic model of the deep drawing metal forming process, suitable for the definition and tuning of a process controller, based on a system model identification procedure. In particular, differently from the state of the art, we model the forming stroke with a single-input multiple-output (SIMO) Hammerstein-Wiener (H-W) model, providing a relationship between the BHF (i.e., the single input) and the draw-in of n different monitored points (i.e., the multiple outputs) around the die. On the other hand, we aim at proposing a proactive control methodology for process control that can provide higher performance with respect to standard controllers. In particular, we propose the application of Model Predictive Control (MPC), demonstrating that, despite its computational complexity, it can be practically applied to the real-time control of fast processes, such as deep drawing. The effectiveness of the proposed process controller is shown on a real case study for a T-shaped metal part using a digital twin (DT) framework, where the performance achieved by the MPC-based system is analyzed in detail and compared against the results obtained through an ad-hoc designed multiple proportional-integral-derivative (PID)-based control architecture.

The paper structure is organized as follows. Section II discusses the state of the art on deep drawing control techniques, focusing on the MPC-based process control approach and positioning the presented approach with respect to the related literature. Section III presents the identification procedure for the process modeling and the consequent definition of the MPC controller. Section IV shows a real case study as a concrete application of the proposed method. Final considerations about the developed work, the implications related to the implementation of the proposed methodology in real scenarios, and future developments are discussed in Section V. In reference to the process addressed in the case study, Appendix A reports the validation performance achieved by the identified model, while Appendix B details the tuning procedure for the employed MPC controller.

II. Literature Review and Paper Positioning

This section reviews the state of the art on process control for deep drawing and describes the contributions of this paper. Since process control recently emerged as a valuable but complex alternative to machine control, the related literature is still limited. In particular, the majority of contributions focus on the modeling of the deep drawing process, while only a few contributions present process control techniques. Among these, we analyse, with particular attention, application of the MPC approach, which reveals to be particularly promising in this context.

A. Process Control of Deep Drawing

In order to properly design an effective process controller for deep drawing, Hsu *et al.*. in [12] indicate two key specifications that must be satisfied. On the one hand, it is essential to model the metal sheet forming in terms of process model, taking into account model uncertainty and process disturbances. This means to properly define a mathematical correlation between the selected input and output process variables. It is also important to consider that the model and its uncertainty are strictly correlated to the specific case study, i.e., it depends on material properties, workpiece shape, press size, and so on. Thus, modeling uncertainty means including small variations in the forming system (such as in blank size and thickness, material properties, and tooling) and external input to the forming system (such as lubrication). On the other hand, the process controller design must guarantee high tracking performance regardless of uncertainties and process disturbance. This means that the control system must satisfy disturbance rejection requirements. Therefore, the literature review presented in the sequel is focused on two main aspects of the deep drawing process control: the models and procedures used for system identification and the techniques adopted for process control, with particular attention to the application of MPC to metal forming.

1) Deep Drawing Models: As it emerges in [13], in deep drawing most of forming variables directly depend on the BHF values during the forming phase. The typical process variables indicated in literature are *wrinkling*, *punch force*, and *draw-in* [1]. The ability to sense the occurrence of wrinkles is potentially useful; however, its measure is limited, because wrinkles locations are not known a priori. Differently, the monitoring of the punch force is more viable and various contributions model the deep drawing process relating the BHF to the punch force [6], [12], [14], [15]. Nevertheless, it is proven that the draw-in of the metal sheet can better reveal the correct execution of the deep drawing process [2], [7]. In fact, more recent works consider the deep drawing process as a relationship between the BHF as input and the draw-in as output. In the related works, the authors aim at obtaining the optimal profile for the BHF and the draw-in of the material via off-line multivariable optimization. The obtained results can then be used as reference signals for process control.

As for deep drawing modeling, two main techniques are viable. On the one hand, the process can be represented considering a physics based modeling approach. This method can be particularly reliable, but also complex and time consuming, considered the non linear nature of the deep drawing process. On the other hand, the process can be considered as a black box and identification procedures can be applied, using linear or nonlinear regression models. In this case the modeling of the system can be less precise with respect to the physics based one, but also simpler and faster, which are valuable features in the industrial sector. Moreover, various assessment tools are available to compare and test the identified models [16] (e.g., *Final Prediction Error (FPE)*, *normalized Akaike's Information Criterion (nAIC)*, and the *Validation Fitting Index (VFI)*). In this way, a more complete and sufficiently exhaustive comparison between different possible solutions is guaranteed.

Although system identification is not a novelty in manufacturing (see e.g., [17]–[19]), to the best of the authors' knowledge, it has never been adopted for the deep drawing process. Indeed, Hsu *et al.* in [6], [12], [14], [15] propose a physics based modeling of the stamping process, where a nonlinear single-input single-output (SISO) first-order dynamical model is obtained considering as input the BHF and as output the punch force. Conversely, in the nonlinear identification context, among several types of nonlinear regression models, the *Nonlinear Auto Regressive eXogenous* (NARX) and the *Hammerstein-Wiener* (H-W) models are largely appreciated for the identification of nonlinear systems [20]–[23]. The former is one of the most traditional nonlinear input-output models, whereas the latter is composed by linear and nonlinear subsystems. Since, the forming process performs a plastic deformation of the material, the workpiece deformation is almost linear until its fracture. This means that non-linearities do not influence the process dynamics under certain conditions. Hence, H-W models can be suitably employed to simplify the representation procedure, considering the process as a hybrid model where it is possible to separately define the non-linear subsystems.

2) PID-Based Process Control: As highlighted in the survey by Allwood *et al.* [13] and in the works [24]–[26], process control aims at improving the overall process performance in the presence of disturbances and ensuring good part quality while preventing process failures. In general, process control architectures present a feedback control loop that controls online the press variables based on the error between process variables and the related reference values. In this context, Hsu *et al.*. in [14], [15] propose the use of PID controllers. In [6], instead, Hsu *et al.*. consider a proportional-integral control with a feed-forward action. Similarly, Lim *et al.*. in [27] propose the use of standard controllers tuned by an automatic controller and some model reference adaptive control approaches. Although the results achieved by the aforementioned works are satisfactory in terms of reference tracking and stamped part quality (also in presence of disturbances), these approaches suffer from the main drawbacks of standard regulators. PID controllers –widely used in several industrial control applications– constitute a good and cheap choice, but they are able to address only simple SISO dynamics. Thus, the application of PID control to multivariable systems requires the definition of ad-hoc control architectures. Moreover, since PIDs cannot properly handle constraints on the

process variables, the tuning phase could be difficult, being heavily dependent on user experience and competency. Thus, the tuning activity can require a large number of tests, often producing sub-optimal control strategies [28].

3) Optimization-Based Process Control: With the aim of overcoming the discussed limits of standard regulators for deep drawing applications, some different strategies have been developed. In particular, more recently thanks to the increase of computing power and the development of novel sensing and actuating technologies, optimal feedback control has gained more attention for the process control of deep drawing. Liu *et al.*. in [29] introduce a process optimal control springback method for the forming monitoring to reduce the springback effect, based on evolutionary strategy. Furthermore, Endelt *et al.*. in [30] propose the optimal control of the BHF by monitoring the draw-in of the metal sheet during the deep drawing phase. They use a non-linear finite element method model for the forming process modelling and a nonlinear least square optimization algorithm for the control system design. In more recent works, a further evolution of optimal control is the proactive approach of MPC [13]. Differently from optimal feedback control, MPC considers the use of a model of the system during the online control to predict the system behavior and compute the most appropriate control actions while optimizing a proper performance indicator. The application of MPC to deep drawing feedback control presents various advantages. First, MPC is a multivariable real-time control strategy that allows driving the outputs of the system by taking into account the interactions between system variables and variables constraints. Then, assuming that a good process model is available, the MPC tuning phase can be carried out in an intuitive and simple way, not necessarily by an expert user. In this context, Hao *et al.*. in [31] and Lu *et al.*. in [32] propose a linear MPC-based process control to monitor the step depth of the workpiece geometrical contour toolpath in incremental sheet forming (ISF). The aim is to reduce the pillow effect, the sheet bending effect, and the springback. It has to be highlighted that the ISF is a progressive sheet metal forming technology where the deformation occurs locally and it is possible to place cameras under the main frame to monitor the sheet metal positions, while this is not possible with the classical deep drawing, where generally sensors have to be positioned around the metal sheet or inside/under the lower/upper die. Moreover, since ISF requires long production time, due to the forming performed with small diameter tools, it is still not particularly suitable for mass production [33] but can benefit of the advantages of the MPC, that is particularly appropriate for slow processes.

B. Paper Contributions

In view of the above discussion, the novelty proposed by this paper is twofold. On the one hand, a multivariable H-W model is obtained in order to describe the deep drawing process. Differently from the state of the art, that generally proposes SISO models putting in relation the BHF and the punch force only, we consider a more complete dynamic model that relates the BHF, as an input, and the draw-in at n different locations around the die, as multiple outputs. The process model is identified considering a black box approach and the obtained H-W model ensures a good compromise between the process controller design easiness and the system representation accuracy. Particularly, this second feature allows an effective evaluation of the performance of the designed process controller by means of simulation tests. On the other hand, we present an MPC-based process control architecture suitable for the proactive real-time control of deep drawing. The MPC-based approach allows the strict fulfillment of the requirements on process variables, thus overcoming the issues discussed previously in Subsection II.A.2. Moreover, thanks to the use of the H-W model, the computation time of the MPC is sufficiently limited and compatible with the short duration of the deep drawing process.

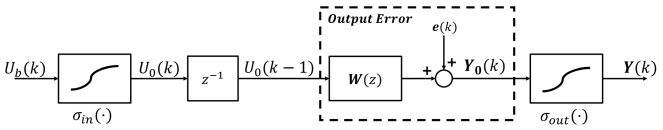

Fig. 4. Block diagram of the Hammerstein-Wiener model representing the nonlinear dynamical process.

III. The Deep Drawing Process Control

In this section we propose the modeling of deep drawing based on nonlinear systems identification, where we consider the BHF as input and the draw-in of n critical points (i.e., points whose dynamics' monitoring can reveal the eventual presence of defects and cracks in the whole stamped part) of the metal sheet profile as output. Subsequently, we provide the definition of an MPC controller for the considered deep drawing process.

A. Process Model Identification

As discussed in the previous section, the draw-in is generally used to extract meaningful information on the state of the forming part. Consequently, we model the deep drawing process as a black box having the BHF (uniformly distributed on the blank holder) as the input variable – denoted as U_b – and the draw-in of n critical points of the metal sheet profile as the output variables – denoted as $\mathbf{Y} = (Y_1, \ldots, Y_n)^\top$ –, thus assuming the system as a SIMO system. In particular, we represent its dynamical behavior by means of a discrete-time nonlinear model, which allows a more precise modeling of the process with respect to possible simplified linearized modeling approaches. More in detail, in this section we propose the use of the H-W model, which describes nonlinear dynamical systems using a linear time-invariant dynamical subsystem sandwiched between two static nonlinear subsystems as illustrated in Fig. 4. The linear SIMO block is represented by a transfer matrix (indicated by $\mathbf{W}(z)$ in Fig. 4), whilst the input and output non-linearities (indicated by functions $\sigma_{in}(\cdot)$ and $\sigma_{out}(\cdot)$ in Fig. 4) are modelled with polynomial estimators:

$$U_0(k) = \sigma_{in}(U_b(k)) \tag{1}$$

$$\mathbf{Y}(k) = \sigma_{out}(\mathbf{Y}_0(k)) \tag{2}$$

where $U_0(k)$ and $\mathbf{Y}_0 = (Y_{01}, Y_{02}, \ldots, Y_{0n})^\top$ are the input and the outputs vector of the SIMO linear subsystem. Note that the transfer matrix $\mathbf{W}(z)$ has the following form:

$$\mathbf{W}(z) = \begin{bmatrix} W_{11}(z) \\ W_{21}(z) \\ \vdots \\ W_{n1}(z) \end{bmatrix} \tag{3}$$

where each element represents the scalar transfer function of the SISO system described by the BHF as input and the draw-in profile of each critical point as output. Alternatively, the SIMO linear subsystem can be reformulated in accordance with the state-space representation:

$$\begin{cases} \mathbf{X_0}(k+1) = \mathbf{A}\mathbf{X_0}(k) + \mathbf{B}U_0(k) \\ \mathbf{Y}_0(k) = \mathbf{C}\mathbf{X_0}(k) + \mathbf{D}U_0(k) \end{cases} \tag{4}$$

where $\mathbf{X}_0 = (\mathbf{X}_1^\top, \mathbf{X}_2^\top, \ldots, \mathbf{X}_n^\top)^\top$ is the state variable vector with $\mathbf{X}_1 = (X_{11}, X_{12}, \ldots, X_{1q})^\top$, $\mathbf{X}_2 = (X_{21}, X_{22}, \ldots, X_{2q})^\top, \ldots, \mathbf{X}_n = (X_{n1}, X_{n2}, \ldots, X_{nq})^\top$, $\mathbf{A}$ is the $(n\,q) \times (n\,q)$ state matrix, $\mathbf{B}$ is the $(n\,q) \times 1$ input matrix, $\mathbf{C}$ is the $n \times (n\,q)$ output matrix, $\mathbf{D}$ is the $n \times 1$ input-output matrix, and q denotes the order of the H-W model.

The model identification procedure requires various preliminary data management steps for a proper data life-cycle, consisting of *Data acquisition*, *Data pre-processing*, and *Data analysis*. Firstly, different experiments must be carried out on the press and, during the forming stroke, real data must be collected, analyzed, integrated, and visualised by using some data management techniques. During the *Data acquisition*, the BHF, i.e., the input variable, and the draw-in at n different points around the die, i.e., the output variables, are collected and stored. We highlight that critical points can change in number and position depending on the shape to be formed. The data retrieved from the press are organized in different datasets suitable for the subsequent steps. Once all data is gathered, following the approach suggested by Baethi *et al.*. in [34] and Tao *et al.*. in [35], a *Data pre-processing* activity must be performed. It consists in the detection of outliers for the data cleaning, a cubic spline interpolation [36] for the data oversampling, and a filtering step by using the Savitzky-Golay filter [37] for the data smoothing. Finally, the *Data analysis* is to be implemented to extract important information from time-series and make them useful by using some visualization data plot and graphics [38].

Finally, we remark that, at the end of the identification procedure, the correctness of the model is proved by simulation, monitoring both its response to the input signal and its output error with respect to the real one. In particular, this phase is also exploited to compare H-W models with a different order p, so that the best performing one is chosen to represent the considered deep drawing process.

B. MPC Design

The proposed MPC-based control system block diagram is reported in Fig. 3. It considers a single MPC block that simultaneously controls the draw-in of the n blank critical points by manipulating the BHF uniformly applied on the whole blank surface. At each sample time, the controller computes the Control Variables (CVs), the State Variables (SVs), and the Output Variables (OVs) related to the given control horizon H_u and prediction horizon H_p respectively in the vector $\mathbf{u}(t) := (U_b(t+1)^\top, \ldots, U_b(t+H_u)^\top)^\top$, $\mathbf{x}(t) := (\mathbf{X}(t+1)^\top, \ldots, \mathbf{X}(t+H_p)^\top)^\top$, and $\mathbf{y}(t) := (\mathbf{Y}_i(t+1)^\top, \ldots, \mathbf{Y}_i(t+H_p)^\top)^\top$. The values of CVs and OVs are subject to physical limitation, as indicated by the following constraints related to time step k:

$$U_b^{\text{lb}} \le U_b(k) \le U_b^{\text{ub}} \tag{5}$$

$$Y_i^{\text{lb}}(k) \le Y_i(k) \le Y_i^{\text{ub}}(k) \quad \forall\, i = 1, \ldots, n \tag{6}$$

where U_b^{lb} and $Y_i^{\text{lb}}(k)$ and U_b^{ub} and $Y_i^{\text{ub}}(k)$ denote the lower and upper bounding for the CVs and the OVs, respectively. The MPC block has the following objective function:

$$\mathbf{J}(\mathbf{u}(t), \mathbf{y}(t)) = \mathbf{J}_{\mathbf{y}}(\mathbf{u}(t), \mathbf{y}(t)) + \mathbf{J}_{\Delta\mathbf{u}}(\mathbf{u}(t), \mathbf{y}(t)). \tag{7}$$

Each term in (7) includes weights (w_i^y and $w^{\Delta u}$) used to balance the competing objectives and described in the sequel. Moreover, Kalman Filter is used as state observer to update the model dynamics at each time step. $\mathbf{J}_{\mathbf{y}}(\mathbf{u}(t), \mathbf{y}(t))$ is the term referring to the output reference tracking and it is defined as follows:

$$\mathbf{J}_{\mathbf{y}}(\mathbf{u}(t), \mathbf{y}(t)) = \sum_{k=t}^{t+H_p-1} \left(\sum_{i=1}^{n} w_i^y \left(Y_i(k+1) - Y_i^{\text{ref}}(k+1) \right)^2 \right)$$

$\mathbf{J}_{\Delta\mathbf{u}}(\mathbf{u}(t), \mathbf{y}(t))$ is the term used for the move suppression controlled variable. During the execution, small CV adjustments (moves) are computed. The MPC controller uses the following scalar performance measure for move suppression controlled variable:

$$\mathbf{J}_{\Delta\mathbf{u}}(\mathbf{u}(t), \mathbf{y}(t)) = \sum_{k=t}^{t+H_u-1} \left(w^{\Delta u} (U(k) - U(k-1))^2 \right).$$

Hence the following optimization problem is solved by the MPC regulator:

$$\min_{\mathbf{u}(k),\, \mathbf{y}(k),\, \mathbf{x}(k)} \mathbf{J}(\mathbf{u}(t), \mathbf{y}(t))$$
$$\text{s. t.} \begin{cases} (1), (2), (4) \;\; \forall k = t+1, \ldots, t+H_p - 1 \\ (5)\, \forall k = t+1, \ldots, t+H_u \\ (6)\, \forall k = t+1, \ldots, t+H_p. \end{cases} \tag{8}$$

More precisely, at each sampling time k, the controller obtains all measurements $\mathbf{y}(k)$, computes the required CVs $\mathbf{u}(k)$ solving (8), and applies to the plant only the first obtained sample.

IV. Case Study

In this section we apply the proposed MPC-based approach to a real case study referred to the manufacturing of the T-shape workpiece shown in Fig. 5.a. This is a structural component of a car bodywork which is realized in HR 440Y580T-FB-UC steel (2 mm thick) and produced at the Gigant company (Bologna, Italy) for Fiat cars.

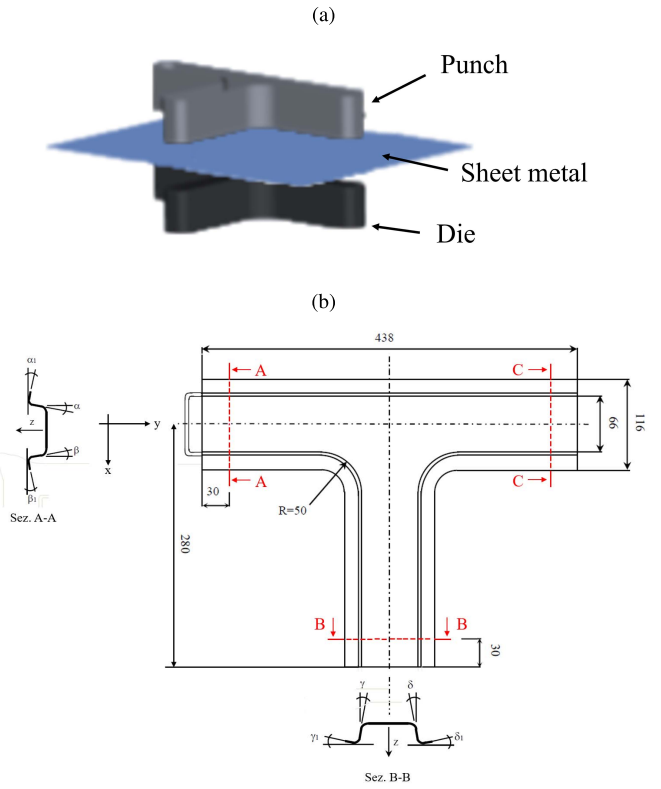

Fig. 5. 'T-shape' steel component: deep drawing mould (a) and mechanical scheme indicating the critical points A, B, and C (b).

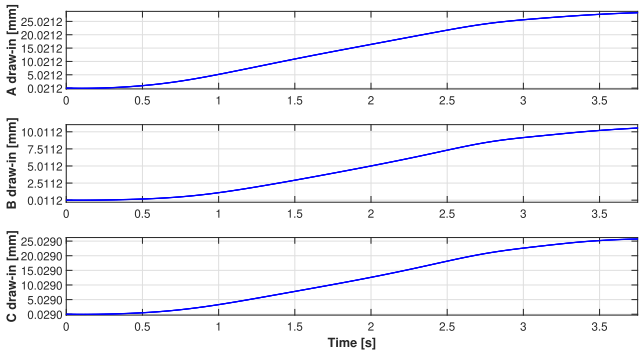

Fig. 6. Draw-in of critical points A, B, and C over time during the forming stroke under the optimal conditions.

A. Setup of Process Control Experiments Based on Digital Twin

The metal forming of the considered component is currently performed using a servo-hydraulic press equipped with a machine controller. The considered press is composed by a sled and a passive pressboard. The sled, surmounted by the upper die, is moved both by a hydraulic axle and an electric axle. Both axles are moved by two actuators: hydraulic pistons are employed for the former, and electric motors for the latter. During the deep drawing phase, only the upper die is pushed down and the BHF acts on the draw-in of the metal sheet. The corresponding complete work-cycle includes five stages (i.e., approach stroke, fluid compression, deep drawing, fluid decompression, and ascent stroke), whose durations are reported in Table I. The core step of the whole forming process is deep drawing: during this phase, the punch runs downwards of 30 mm providing a stroke at a speed of 8 mm/s. The total load, provided by each single hydraulic actuator, remains constant. In this step only the hydraulic axle works, but the electric axle can allow a force adjustment within a small range of values, overlapping with the force transmitted by hydraulic pistons to the sled. Table II shows the technical specifications of the hydraulic piston utilized as actuator during the deep drawing phase. Since the electrical axis can work during this step (if necessary), the maximum force available to the sled is equal to $(2 \times 1500) + 280$ kN $= 3280$ kN.

TABLE I
SERVO-HYDRAULIC PRESS WORK-CYCLE: STEPS AND CORRESPONDING DURATIONS

	Step	Duration [s]
	Approach stroke	2.39
	Fluid compression	0.42
	Deep drawing	3.88
	Fluid decompression	0.26
	Ascent stroke	2.70
Tot. time		9.66

TABLE II
TECHNICAL SPECIFICATION OF THE HYDRAULIC PISTON

Parameter	Unit	Value
N. of hydraulic actuators	-	2
Max. force per single actuator	kN	1500
Sensitivity	kN	± 60
Response time	ms	100
Speed	m/s	8

In the framework of a research project aimed at implementing Industry 4.0 paradigms, the press is being enhanced by adding a process controller. To this aim, on the one hand, the press has been equipped with three laser displacement sensors aimed at measuring in real-time the draw-in of the metal sheet edge in the critical points A, B, and C illustrated in Fig. 5.b, during the stamping process. Note that the choice of these points is the result of a robust off-line multivariable optimization based on stamping experiments and numerical simulations conducted on the addressed process. As an additional outcome of this analysis, the optimal draw-in profiles for the critical points A, B, and C are determined in reference to the optimal BHF – denoted as U_b^{ref} – equal to 588 kN (see Fig. 6). On the other hand, the process controller has been designed in accordance to the methodology described in Section III and has been tested in a DT framework described in the sequel. The sampling time is set to 200 ms. Note that the detailed features of the identified model are described in Appendix A, whilst the performance of the designed MPC controller as well as the values of parameters are reported in Appendix B.

In the Industry 4.0 framework, the use of the DT is widely adopted, especially in the manufacturing and automotive context [39], [40]. In effect, the development of a cyber-physical system in addition to the deployment of a complex network of DT interacting with monitored and controlled elements is

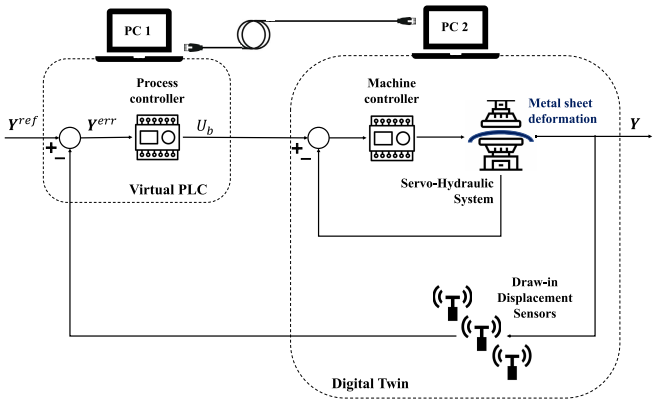

Fig. 7. Software-in-the-loop framework used for the closed-loop MPC-based control system simulation.

an important key enabling technology for the optimal design, commissioning, and maintenance of stamping presses [41]. In fact, especially in the context of production systems commissioning, the DT is commonly used to leverage on the benefit derived from the recent concept of Virtual Commissioning (VC). VC enables the full validation and verification of a complex manufacturing system by performing a simulation involving a virtual plant and a real controller, thus reducing the time to market, lowering costs, and increasing productivity [42]. Simulations based on a Software-in-the-loop (SWIL) approach are generally used to virtually test the control system before the physical implementation of the plant is finished [43], [44]. Following this trend, in this case study a SWIL simulation -based architecture is employed to test the proposed closed-loop control system, using the DT of the press instead of its physical implementation. Figure 7 shows the complete architectural framework implemented for the SWIL simulation of the deep drawing control system. In particular, the designed MPC algorithm is implemented in a virtual Programmable Logic Controller (PLC) that is in turn deployed on the PC1 digital platform: here the process controller runs, computing the optimal BHF and communicating such a control action (i.e., U_b) to the inner machine control loop. Viceversa, the PC2 digital platform is dedicated to the DT of the press including the digital models of the servo-hydraulic system, the deep drawing process (i.e., the metal sheet that is getting deformed), the machine controller, and the three draw-in displacement sensors. The communication between PC1 and PC2 is based on the Open Platform Communications Unified Architecture (OPC UA), whilst the communication between PC1 and the DT of the sensors is managed by the Transmission Control Protocol/Internet Protocol (TCP/IP). The PLC used for the virtual simulation is the Siemens S7-1500 with CPU 1515T-2 PN, programmed in the TIA Portal V15 environment, while the virtual commissioning of the PLC is performed using the S7-PLCSIM Advanced V3.0 software [45].

B. MPC Controller Results Analysis

By using the SWIL simulation framework shown in Fig. 7, the MPC-based closed-loop control system tuned as described in Appendix B is simulated. The effectiveness of the proposed control method is tested considering the closed-loop system reference trajectory tracking capability. Thus, the BHF error with respect to the optimal value U_b^{ref} (i.e., 588 kN) is obtained as $U_b^{err} = (U_b^{ref} - U_b)$, while the draw-in error with respect to the reference value $\mathbf{Y}^{ref}$ is obtained as $\mathbf{Y}^{err} = (\mathbf{Y}^{ref} - \mathbf{Y})$. In all simulations, external process disturbances are taken into account by considering a step disturbance affecting the control input and characterized by an amplitude equal to 4% of the reference value U_b^{ref}.

The experimental results are reported in Fig. 8. In particular, Fig. 8.a shows the reference trajectory tracking capability, while Fig. 8.b the output error trajectory tracking. More in detail, the components of the error vector $\mathbf{Y}^{err}$ (i.e., Y_i^{err} for $i = \{1, 2, 3\}$ indicating the error between the actual and the reference draw-in at the critical points A, B, and C) get the mean values of 0.9%, 0.8%, and 0.7%, respectively. The BHF reference trajectory tracking error U_b^{err} is 0.1%. It is worthwhile noting that the obtained draw-in errors (indicated by dotted curves in Fig. 8.b) are inside the tolerance band (represented by shaded area bounded by the dashed lines in Fig. 8.b), thus ensuring that the stamped workpiece is defect free, despite the presence of the modeled external disturbances.

Finally, a Monte Carlo simulation with 1000 runs is carried out in order to validate the runtime performance of the deployed control system in the SWIL framework described above. In reference to a single sampling period, the mean and maximum values of the main computational and communication efforts (i.e., the actual sampling time, the MPC algorithm elaboration time, the TCP/IP, and OPC UA communication delays) are reported in Table III, demonstrating that, despite its computational complexity, the approach can be practically applied for the real-time control of fast processes.

TABLE III
MPC-BASED CONTROL SYSTEM COMPUTATIONAL AND COMMUNICATION PERFORMANCE OVER MONTE CARLO SIMULATIONS

	$\mathbf{T_s}$ [ms]	TCP/IP delay [ms]	MPC computation time [ms]	OPC UA delay [ms]
Mean	213.1	29.1	1.8	9.5
Maximum	215.8	34.0	2.8	15.1

C. Comparison With a Multiple PID-Based Control Architecture

With the aim of evaluating and better highlighting the advantages of our approach with respect to the related literature, we provide a comparison between the results obtained by the proposed technique and those achieved by a baseline method, using the PID control approach. To this aim, since the forming process is identified as a SIMO system, a custom multiple PID-based control architecture, whose block diagram is shown in Fig. 10, is used for the comparison analysis. Each $\text{PID}_i(z)$ (with $i = 1, 2, 3$) – in series to a saturation block – computes a PID time-discrete control action contributing to

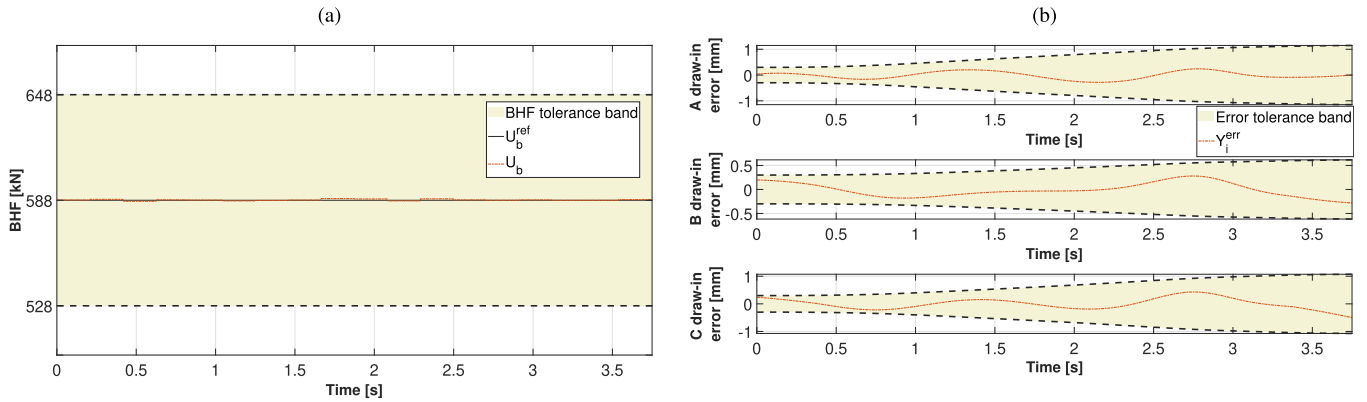

Fig. 8. MPC-based control system results: BHF profile vs. bounding range (a); draw-in error profile of critical points A, B, and C vs. tolerance band (b).

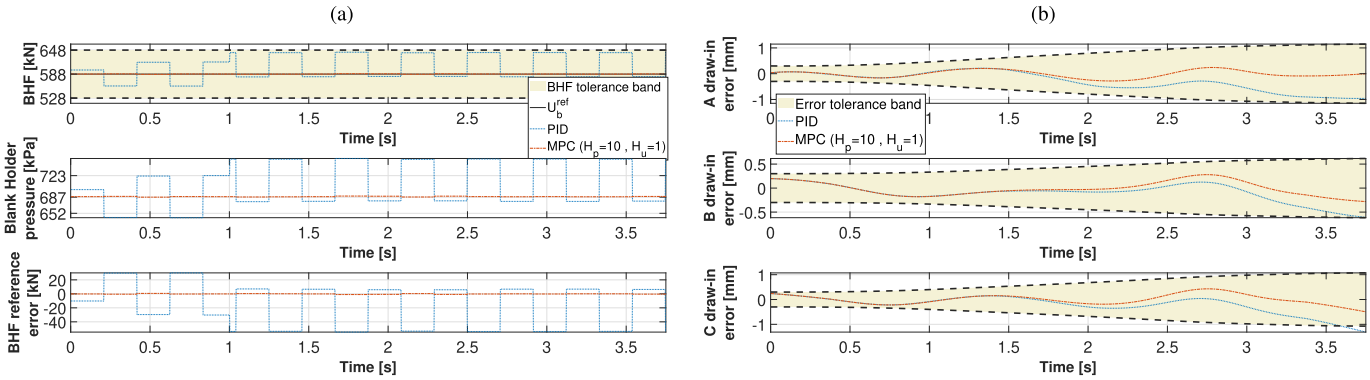

Fig. 9. Closed-loop system response comparison between the multiple PID-based and the MPC-based ($H_p = 10$, $H_u = 1$) controllers. Input reference tracking capability (a) and output error of critical points A, B, and C vs. tolerance band (b).

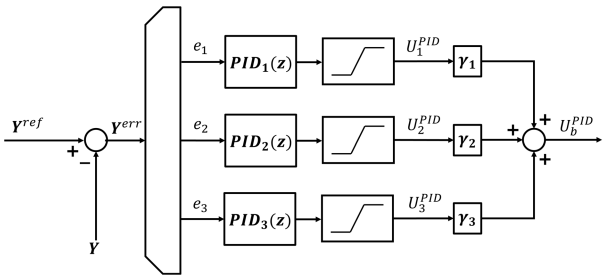

Fig. 10. Block diagram of the proposed multiple PID-based controller architecture.

the overall control input $U_b^{ref}(k)$ (i.e., the BHF) as follows:

$$U_b^{PID}(k) = \gamma_1 U_1^{PID}(k) + \gamma_2 U_2^{PID}(k) + \gamma_3 U_3^{PID}(k) \quad (9)$$

where γ_1, γ_2, and γ_3 are weighting factors adopted in the linear combination. Note that, in this approach, the metal forming process is considered as composed by n different SISO systems (one for each measured draw-in and identified with a H-W model) that have to be controlled individually. The tuning phase of this PID-based controller has a twofold drawback. On the one hand, the tuning is required for each subsystem, resulting in an effort increase. On the other hand, the final control action needed by the whole system has to be determined through a proper weighted sum represented by Eq. (9), where the weights have to be appropriately determined. This implies the execution of a non negligible *trial-and-error* procedure which contributes to making the tuning phase difficult. Morever, the tuned parameters must be modified whenever any characteristic of the plant changes, resulting in a non scalable architecture, in contrast with the MPC approach. These considerations imply that the tuning phase of the PID-based controller is definitely harder than the MPC design.

The PID-based controller described above is tested in the DT control architecture shown in Fig. 7, where the MPC controller is replaced by the PID controller. Also in this case, a step disturbance affecting the control input and characterized by an amplitude equal to 4% of the reference value is considered. Figure 9 shows the different closed-loop control responses obtained by the multiple PID-based controller against the MPC based controller. From the results comparison it is evident that the PID-based controller does not guarantee a robust closed-loop stability and an albeit small deviation of the BHF with respect to the optimal trajectory U_b^{ref} occurs (Fig. 9.a). Not surprisingly, the benefit of the proposed MPC methodology is to include the machine control loop into the process control closed-loop in order to perform a constant BHF reference value for the inner loop as the machine controller operates, and achieve the desired draw in trajectories. Indeed, as shown in Fig. 9, the MPC-based process control allows keeping the errors related both to the control output within the tolerance band (represented by the shaded area in the

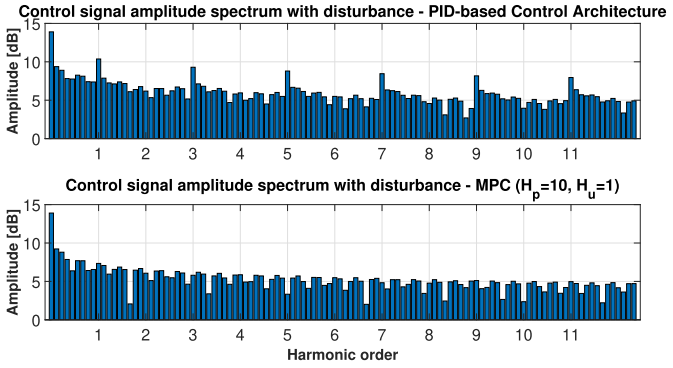

Fig. 11. BHF FFT amplitudes spectrum comparison between the PID-based and MPC-based controllers.

figure) better than the PID-based approach. In addition, it is worthwhile noting that in the case of the PID-based approach the draw-in error of the critical point C goes out of the band (see the bottom subplot in Fig. 9.b). Moreover, the BHF value computed by the process controller does not oscillate around the reference value, leading a higher closed-loop stability than the multiple PID case. Finally, we remark that the MPC based control system requires a lower control effort than the multiple PID-based approach. To this aim, the comparison of the control effort of the BHF signal obtained by the multiple PID and the MPC -based control system is analyzed using the Fast Fourier Transformation (FFT). Analyzing the FFT amplitude spectra reported in Fig. 11, it is apparent that the high-order harmonics content obtained by the MPC approach is more moderate than the one achieved by the PID-based one, thus its control effort is lower.

V. Conclusion and Future Works

In this paper we propose a Model Predictive Control (MPC) based approach for cold sheet metal forming, which aims at optimizing the process in terms of stamped objects quality. A comprehensive methodology is developed in detail, ranging from process modeling (model identification and validation based on experimental data acquisition) to MPC implementation (control architecture definition and controller tuning and testing).

The paper contribution is twofold. On the one hand, the proposed approach fills a gap in the existing literature, where –in reference to metal forming– classical controllers (such as Proportional-Integral-Derivative) are commonly employed, even though they cannot properly handle constraints and require a difficult tuning phase, thus not always producing an optimal control signal. Conversely, the proposed approach achieves an excellent control quality of a multivariable constrained process under a simple fast tuning phase and short controlling time period. On the other hand, the application to a deep drawing real press highlights the effectiveness of the proposed methodology in designing a suitable control system able to make the stamped parts free of defects. Finally, using a digital twin model of the press (including the servo-hydraulic system, the deep drawing process, the machine controller, and the sensors), the practical feasibility of the MPC controller is demonstrated in a real-time software-in-the-loop (SWIL) simulation, despite the computational complexity and the fast dynamics of the involved process.

Future works will be devoted to the implementation and testing of the designed control systems in real experiments using a physical controller platform (instead of the SWIL) and the physical press (instead of its digital model). Future developments will also be focused on extending the proposed approach to other promising MPC schemes, such as explicit MPC, which allows reducing the computational time needed to determine the control actions compared to implicit MPC. Another research development could be the investigation of the proactive integration of the process controller into prognostic and health management (PHM) systems. For instance, using adaptive MPC-based techniques could bring the PHM system to autonomously understanding the optimal operating conditions, providing the process controller with a time-varying reference trajectory.

TABLE IV
Mean Value and Variance of Time-Series That Compose the Training and the Validation Datasets

		Mean value [mm]	Variance [mm]
Training dataset	draw-in A	14.4708	110.3194
	draw-in B	4.8239	15.5817
	draw-in C	12.1045	92.4157
Validation dataset	draw-in A	14.4580	110.5453
	draw-in B	4.8443	15.6440
	draw-in C	12.0870	92.4777

Appendix A
Identification of the Deep Drawing Process Addressed by the Case Study

For the sake of identifying the deep drawing process model, several experiments are conducted in accordance with three different values of the BHF (i.e., 400, 700, and 588 kN) on the press: the draw-in of the A, B, and C critical points (Fig. 5.b), during the deep drawing phase, are measured and recorded. It is important to point out that the duration of each phase, reported in Table I, is indicative. Specifically, for the experiments related to the considered workpiece (see Fig. 5.a), the duration of the deep drawing phase (step 3 of the press work-cycle) is 3.75 s on average and a stroke of 30 mm at a speed of 8 mm/s is run on average by the punch. First, the collected data are arranged in a training and validation dataset, one per each experiment. As shown in Table IV, both training and validation datasets have the same statistics, thus confirming the correctness of the datasets definition.

Subsequently, as indicated in Section III.A, an identification analysis is performed in order to define the parameters of the H-W representing the considered deep drawing process. In particular, the analyzed process is suitably identified through a second-order H-W model, i.e., $p = 2$. The input and output non-linear functions indicated by $\sigma_{in}(\cdot)$ and $\sigma_{out}(\cdot)$ (Fig. 4), respectively, are modelled with a first-degree polynomial, whilst the transfer matrix $\mathbf{W}(z)$ of the linear SIMO block given

in (3) is obtained as follows:

$$\mathbf{W}(z) = \begin{bmatrix} \dfrac{-0.98z^{-1} - z^{-2}}{1 - 1.99z^{-1} + 0.99z^{-2}} \\ \dfrac{-0.93z^{-1} - z^{-2}}{1 - 1.99z^{-1} + z^{-2}} \\ \dfrac{-0.95z^{-1} - z^{-2}}{1 - 1.99z^{-1} + z^{-2}} \end{bmatrix} \tag{10}$$

where each element represents the transfer function of each SISO system described by the BHF as input and the A, B, and C draw-in profiles as outputs. Both numerator and denominator polynomials have second order, since the model is of the second order. From the output-error polynomial form of the linear SIMO block, the corresponding state-space representation given in (4) is obtained as follows:

$$\begin{cases} \mathbf{X}_0(k+1) = \mathbf{A}\mathbf{X}_0(k) + \mathbf{B}U_0(k) \\ \mathbf{Y}_0(k) = \mathbf{C}\mathbf{X}_0(k) + \mathbf{D}U_0(k) \end{cases} \tag{11}$$

where $\mathbf{X}_0 = [\mathbf{X}_A^\top, \mathbf{X}_B^\top, \mathbf{X}_C^\top]^\top$ is the state variable vector with $\mathbf{X}_A = (X_{A1}, X_{A2})^\top$, $\mathbf{X}_B = (X_{B1}, X_{B2})^\top$, $\mathbf{X}_C = (X_{C1}, X_{C2})^\top$, $\mathbf{Y}_0 = (Y_A, Y_B, Y_C)^\top$ is the output vector, and U_0 is the input. $\mathbf{A}$ is the 6×6 state matrix, $\mathbf{B}$ is the 6×1 input matrix, $\mathbf{C}$ is the 3×6 output matrix, and $\mathbf{D}$ is the 3×1 input-output matrix, defined as:

$$\mathbf{A} = \begin{bmatrix} 0.999 & 0.002 & 0 & 0 & 0 & 0 \\ -0.002 & 0.999 & 0 & 0 & 0 & 0 \\ 0 & 0 & 1 & 0.002 & 0 & 0 \\ 0 & 0 & -0.002 & 1 & 0 & 0 \\ 0 & 0 & 0 & 0 & 1 & 0.002 \\ 0 & 0 & 0 & 0 & -0.002 & 0.999 \end{bmatrix}$$

$$\mathbf{B} = \begin{bmatrix} 0.3537 \\ -0.001 \\ 0.354 \\ 447.400 \\ 0.354 \\ 429.300 \end{bmatrix}$$

$$\mathbf{C} = \begin{bmatrix} -2.80 & -32.12 & 0 & 0 & 0 & 0 \\ 0 & 0 & 0.096 & -0.002 & 0 & 0 \\ 0 & 0 & 0 & 0 & 0.066 & -0.002 \end{bmatrix}$$

$$\mathbf{D} = \begin{bmatrix} 0 \\ 0 \\ 0 \end{bmatrix}. \tag{12}$$

The H-W model described above is implemented in the *Matlab* engineering software using the Identification Toolbox. With the aim of highlighting the advantages of the second order H-W model with respect to other approaches, we provide a comparison with the results obtained by the NARX model. The comparison results are shown in Figs. 12 and 13. Even though the NARX model fits the validation dataset with a confidence of 100% (see Fig. 12), it suffers from over-parameterization, due to the inherent structural-identifiability issue of this class of models. In fact, as shown in Fig. 13, the second-order H-W model has a higher close-fitting simulated response compared with respect to the NARX model. For each

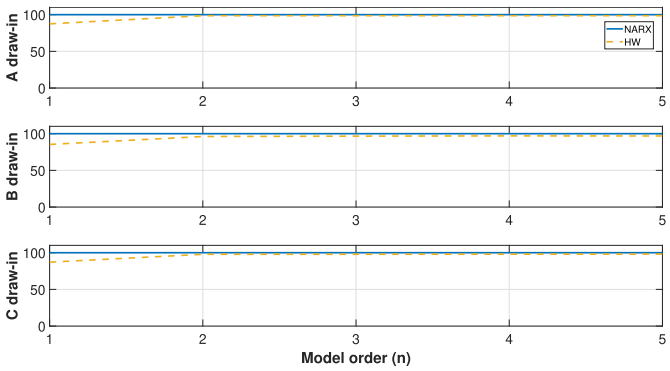

Fig. 12. Validation fitting index comparison between the H-W and the NARX identified models.

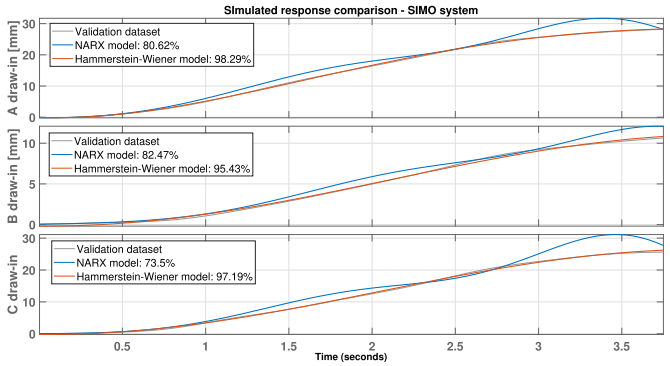

Fig. 13. Simulated response comparison between the H-W and the NARX identified models.

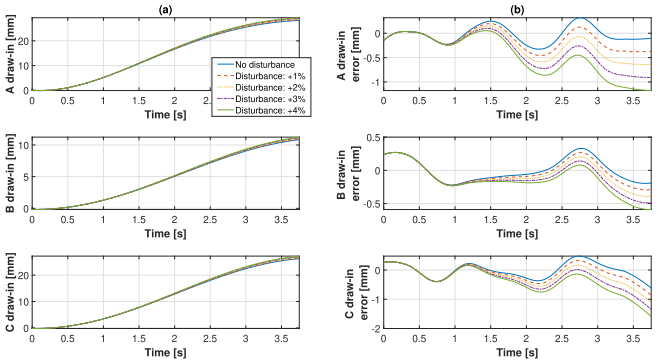

Fig. 14. System simulated response comparison (a) and draw-in errors (b) in presence of a step disturbance (amplitude equal to 1%, 2%, 3%, and 4% of the BHF value).

draw-in output, the H-W model presents a behaviour that is very similar to the actual one.

Moreover, as a further validation analysis, an external disturbance is superimposed to the input BHF used in the deep drawing process. Figure 14 shows the results obtained by the system simulation conducted using a disturbance step with increasing amplitude (1%, 2%, 3%, and 4% of the input BHF value). As expected, the results demonstrate the advantages of a closed-loop control system for the metal forming process. Conversely, in Fig. 15 the simulated system responses are shown for a BHF whose value corresponds to different working conditions (i.e., 400 kN and 700 kN). It is apparent

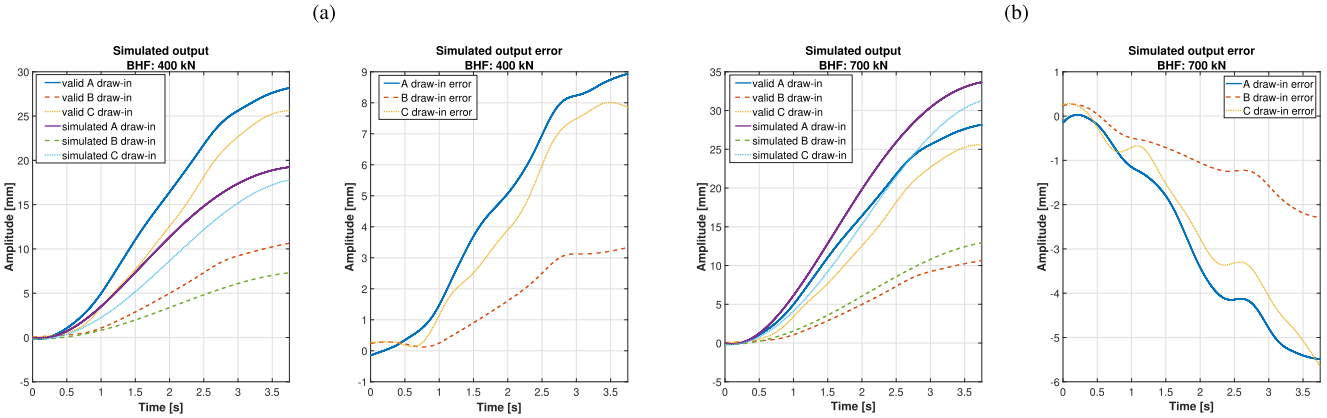

Fig. 15. Simulated outputs and output errors for the identified SIMO system with an input BHF equal to of 400 kN (a) and 700 kN (b).

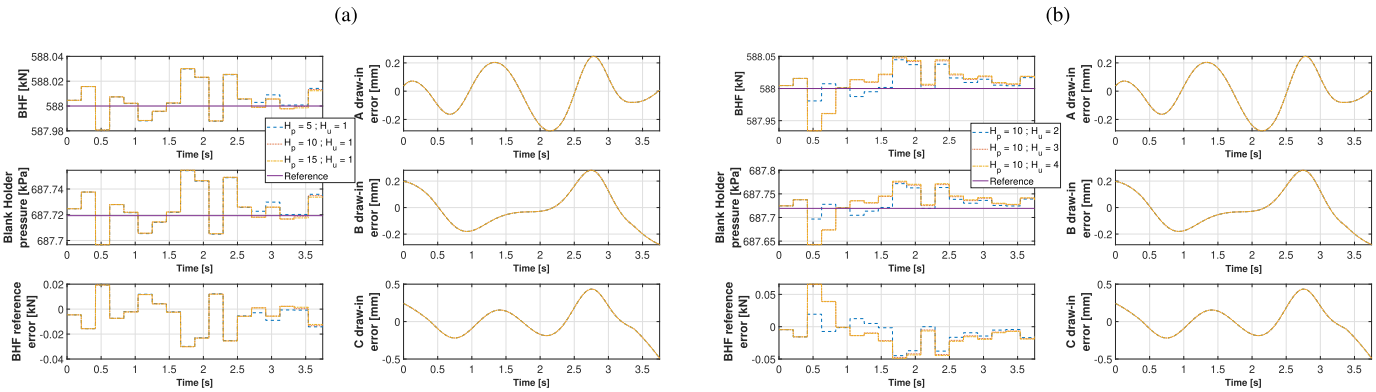

Fig. 16. MPC Closed-loop system response for $H_u = 1$ and $H_p = (5, 10, 15)$ (a) and for $H_p = 10$ and $H_u = (2, 3, 4)$ (b).

TABLE V
MPC INPUT AND OUTPUT CONSTRAINTS

Parameter	Unit	Value
U_b^{lb}, U_b^{ub}	kN	528, 648
$Y_1^{lb}(k)$, $Y_1^{ub}(k)$	mm	$(1-\alpha)Y_1^{ref}(k)$, $(1+\alpha)Y_1^{ref}(k)$
$Y_2^{lb}(k)$, $Y_2^{ub}(k)$	mm	$(1-\alpha)Y_2^{ref}(k)$, $(1+\alpha)Y_2^{ref}(k)$
$Y_3^{lb}(k)$, $Y_3^{ub}(k)$	mm	$(1-\alpha)Y_3^{ref}(k)$, $(1+\alpha)Y_3^{ref}(k)$

TABLE VI
MPC PARAMETERS

Parameter	Unit	Value
H_p	-	10
H_u	-	1
T_s	ms	200
w_1^y	-	1
w_2^y	-	1
w_3^y	-	1
$w^{\Delta u}$	-	0
α	-	0.03

that the obtained H-W model correctly represents the metal forming process only when the BHF gets the nominal value (i.e., 588 kN). In fact, for a lower value of BHF (Fig. 15.a), the model tends to under-estimate its response, while in the case of a BHF value of 700 kN (Fig. 15.b), the model tends to over-estimate its response.

APPENDIX B
TUNING OF THE MPC CONTROLLER FOR THE CASE STUDY

The MPC-based process controller defined by (8) is designed and tuned with the *MATLAB MPC Designer*, inheriting the structure of the identified process in the scheme of Fig. 4.

The input constraints are limited by the hydraulic piston sensitivity (±60 kN), while the output constraints are limited within a tolerance band centered in the optimal draw-in profiles Y_1^{ref}, Y_2^{ref}, and Y_3^{ref}. The tolerance band is defined by parameter α, whose value is an outcome of the robust analysis of the stamping experiments. All the constraint parameters values are reported in Table V. The values of the other MPC parameters (i.e., H_p, and H_u, the variables weights, the variables rate weights, and α) are detailed in Table VI. The MV nominal input value U_b is fixed at 588 kN and for the output reference trajectory (indicated as Y_1^{ref}, Y_2^{ref}, and Y_3^{ref}) the optimal draw-in displacement shown in Fig. 6 is considered. Moreover, since the inner machine control loop works with two hydraulic pistons having a response time of 100 ms, the MPC-based process controller sampling time T_S is settled at 200 ms. With regard to the control horizon H_p and the prediction horizon H_u, since they are considered as tuning parameters, their changes are evaluated during the testing phase. Figure 16.a shows

the closed-loop control system simulation for three different values of prediction horizon ($H_p = \{5, 10, 15\}$) and a constant value of control horizon ($H_u = 1$), while Fig. 16.b illustrates the closed-loop system dynamics for increasing values of the control horizon ($H_u = \{2, 3, 4\}$) and a constant value of the prediction horizon ($H_p = 10$). Changes in H_p does not affect the behaviour of the input variable, whereas, as H_u grows, the CV signal tends to be more and more oscillating around the nominal value.

ACKNOWLEDGMENT

The authors would like to thank the CRF (Centro Ricerche Fiat) S.p.A. Staff for their support in the preparation of this article, the SMATI (materials and innovative technology) Research Group of the Polytechnic of Bari (Italy) for their provision of experimental data, and the Gigant S.r.l. Company for the press specification and tests.

REFERENCES

[1] Y. Lim, A. G. Ulsoy, and R. Venugopal, *Process Control for Sheet-Metal Stamping*. Cham, Switzerland: Springer, 2013.

[2] M. E. Palmieri, V. D. Lorusso, and L. Tricarico, "Robust optimization and Kriging metamodeling of deep-drawing process to obtain a regulation curve of blank holder force," *Metals*, vol. 11, no. 2, p. 319, Feb. 2021.

[3] K. Gopalakrishnan *et al.*, "Unilateral fixtures for sheet-metal parts with holes," *IEEE Trans. Autom. Sci. Eng.*, vol. 1, no. 2, pp. 110–120, Oct. 2004.

[4] Y.-M. H. N. M. Y. Y. H. R. Du, "Diagnosis of sheet metal stamping processes based on 3-D thermal energy distribution," *IEEE Trans. Autom. Sci. Eng.*, vol. 4, no. 1, pp. 22–30, Jan. 2007.

[5] W. Sheng, H. Chen, N. Xi, and Y. Chen, "Tool path planning for compound surfaces in spray forming processes," *IEEE Trans. Autom. Sci. Eng.*, vol. 2, no. 3, pp. 240–249, Jul. 2005.

[6] C.-W. Hsu, A. G. Ulsoy, and M. Y. Demeri, "Development of process control in sheet metal forming," *J. Mater. Process. Technol.*, vol. 127, no. 3, pp. 361–368, Oct. 2002.

[7] C. Su, K. Zhang, S. Lou, T. Xu, and Q. Wang, "Effects of variable blank holder forces and a controllable drawbead on the springback of shallow-drawn TA2M titanium alloy boxes," *Int. J. Adv. Manuf. Technol.*, vol. 93, nos. 5–8, pp. 1627–1635, Nov. 2017.

[8] M. Dotoli, A. Fay, M. Miśkowicz, and C. Seatzu, "An overview of current technologies and emerging trends in factory automation," *Int. J. Prod. Res.*, vol. 57, nos. 15–16, pp. 5047–5067, Aug. 2019.

[9] G. Cavone, N. Epicoco, and M. Dotoli, "Process re-engineering based on colored Petri nets: The case of an Italian textile company," in *Proc. 28th Medit. Conf. Control Autom. (MED)*, Sep. 2020, pp. 856–861.

[10] K. Siegert, M. Ziegler, and S. Wagner, "Closed loop control of the friction force. Deep drawing process," *J. Mater. Process. Technol.*, vol. 71, no. 1, pp. 126–133, Nov. 1997.

[11] A. Bozza, G. Cavone, R. Carli, L. Mazzoccoli, and M. Dotoli, "An MPC-based approach for the feedback control of the cold sheet metal forming process," in *Proc. IEEE 17th Int. Conf. Autom. Sci. Eng. (CASE)*, Aug. 2021, pp. 286–291.

[12] C.-W. Hsu, A. G. Ulsoy, and M. Y. Demeri, "An approach for modeling sheet metal forming for process controller design," *J. Manuf. Sci. Eng.*, vol. 122, no. 4, pp. 717–724, Nov. 2000.

[13] J. M. Allwood *et al.*, "Closed-loop control of product properties in metal forming," *CIRP Ann.*, vol. 65, no. 2, pp. 573–596, 2016.

[14] C.-W. Hsu, A. Ulsoy, and M. Demeri, "Process controller design for sheet metal forming," in *Proc. Amer. Control Conf.*, vol. 1, 1999, pp. 192–196.

[15] C.-W. Hsu, A. G. Ulsoy, and M. Y. Demeri, "An approach for modeling sheet metal forming for process controller design," *J. Manuf. Sci. Eng.*, vol. 122, no. 4, pp. 717–724, Nov. 2000.

[16] L. Ljung, "System identification," in *Signal Analysis and Prediction*. Springer, 1998, pp. 163–173.

[17] L. T. Tunc and E. Budak, "Identification and modeling of process damping in milling," *J. Manuf. Sci. Eng.*, vol. 135, no. 2, Apr. 2013, Art. no. 021001, doi: 10.1115/1.4023708.

[18] P. Rao, S. Bukkapatnam, O. Beyca, Z. Kong, and R. Komanduri, "Real-time identification of incipient surface morphology variations in ultraprecision machining process," *J. Manuf. Sci. Eng.*, vol. 136, no. 2, Apr. 2014, Art. no. 021008, doi: 10.1115/1.4026210.

[19] P. M. Sammons, D. A. Bristow, and R. G. Landers, "Two-dimensional modeling and system identification of the laser metal deposition process," *J. Dyn. Syst., Meas., Control*, vol. 141, no. 2, Feb. 2019, Art. no. 021012, doi: 10.1115/1.4041444.

[20] A. Perrusquía and W. Yu, "Identification and optimal control of nonlinear systems using recurrent neural networks and reinforcement learning: An overview," *Neurocomputing*, vol. 438, pp. 145–154, May 2021.

[21] J. Li, W. X. Zheng, J. Gu, and L. Hua, "A recursive identification algorithm for Wiener nonlinear systems with linear state-space subsystem," *Circuits, Syst., Signal Process.*, vol. 37, no. 6, pp. 2374–2393, Jun. 2018.

[22] W. Zhao, W. X. Zheng, and E.-W. Bai, "A recursive local linear estimator for identification of nonlinear ARX systems: Asymptotical convergence and applications," *IEEE Trans. Autom. Control*, vol. 58, no. 12, pp. 3054–3069, Dec. 2013.

[23] W. X. Zhao, H. F. Chen, and W. X. Zheng, "Recursive identification for nonlinear ARX systems based on stochastic approximation algorithm," *IEEE Trans. Autom. Control*, vol. 55, no. 6, pp. 1287–1299, Jun. 2010.

[24] B. A. Rashap *et al.*, "Control of semiconductor manufacturing equipment: Real-time feedback control of a reactive ion etcher," *IEEE Trans. Semicond. Manuf.*, vol. 8, no. 3, pp. 286–297, Aug. 1995.

[25] A. G. Ulsoy, Y. Koren, and F. Rasmussen, "Principal developments in the adaptive control of machine tools," *J. Dyn. Syst., Meas., Control*, vol. 105, no. 2, pp. 107–112, Jun. 1983.

[26] A. G. Ulsoy and Y. Koren, "Control of machining processes," *J. Dyn. Syst., Meas. Control, Trans. ASME*, vol. 115, no. 2B, pp. 301–308, 1993.

[27] Y. Lim, R. Venugopal, and A. G. Ulsoy, "Auto-tuning and adaptive control of sheet metal forming," *Control Eng. Pract.*, vol. 20, no. 2, pp. 156–164, Feb. 2012.

[28] R. P. Borase, D. Maghade, S. Sondkar, and S. Pawar, "A review of PID control, tuning methods and applications," *Int. J. Dyn. Control.*, vol. 9, no. 2, pp. 1–10, 2020.

[29] W. Liu, Z. Liang, T. Huang, Y. Chen, and J. Lian, "Process optimal control of sheet metal forming springback based on evolutionary strategy," in *Proc. 7th World Congr. Intell. Control Autom.*, 2008, pp. 7940–7945.

[30] B. Endelt, S. Tommerup, and J. Danckert, "A novel feedback control system–controlling the material flow in deep drawing using distributed blank-holder force," *J. Mater. Process. Technol.*, vol. 213, no. 1, pp. 36–50, Jan. 2013.

[31] W. Hao and S. Duncan, "Constrained model predictive control of an incremental sheet forming process," in *Proc. IEEE Int. Conf. Control Appl. (CCA)*, Sep. 2011, pp. 1288–1293.

[32] H. Lu, M. Kearney, Y. Li, S. Liu, W. J. T. Daniel, and P. A. Meehan, "Model predictive control of incremental sheet forming for geometric accuracy improvement," *Int. J. Adv. Manuf. Technol.*, vol. 82, nos. 9–12, pp. 1781–1794, Feb. 2016.

[33] J. Pathak, "A brief review of incremental sheet metal forming," *Int. J. Latest Eng. Manage. Res.*, vol. 2, no. 3, pp. 35–43, 2017.

[34] R. Baheti and H. Gill, "Cyber-physical systems," *Impact Control Technol.*, vol. 12, pp. 161–166, Mar. 2011.

[35] F. Tao, J. Cheng, Q. Qi, M. Zhang, H. Zhang, and F. Sui, "Digital twin-driven product design, manufacturing and service with big data," *Int. J. Adv. Manuf. Technol.*, vol. 94, nos. 9–12, pp. 3563–3576, 2018.

[36] C. De Boor, *A Practical Guide to Splines*. New York, NY, USA: Springer-Verlag, 1978.

[37] A. Savitzky and M. J. E. Golay, "Smoothing and differentiation of data by simplified least squares procedures," *Anal. Chem.*, vol. 36, no. 8, pp. 1627–1639, Jul. 1964.

[38] S. Keivanpour and D. A. Kadi, "Strategic eco-design map of the complex products: Toward visualisation of the design for environment," *Int. J. Prod. Res.*, vol. 56, no. 24, pp. 7296–7312, Dec. 2018.

[39] R. Rosen, G. Von Wichert, G. Lo, and K. D. Bettenhausen, "About the importance of autonomy and digital twins for the future of manufacturing," *IFAC-Papers OnLine*, vol. 48, no. 3, pp. 567–572, 2015.

[40] J. Vachálek, L. Bartalskỳ, O. Rovnỳ, D. Šišmišová, M. Morháč, and M. Lokšík, "The digital twin of an industrial production line within the Industry 4.0 concept," in *Proc. 21st Int. Conf. Process Control (PC)*, Jun. 2017, pp. 258–262.

[41] R. Carli, G. Cavone, M. Dotoli, N. Epicoco, C. Manganiello, and L. Tricarico, "ICT-based methodologies for sheet metal forming design: A survey on simulation approaches," in *Proc. IEEE Int. Conf. Syst., Man Cybern. (SMC)*, Oct. 2019, pp. 128–133.

[42] S. Fur, O. Riedel, and A. Verl, "Hybrid commissioning of production plants," in *Proc. 26th IEEE Int. Conf. Emerg. Technol. Factory Autom. (ETFA)*, Sep. 2021, pp. 1–6.
[43] M. Scholz, S. Oberschachtsiek, T. Donhauser, and J. Franke, "Software-in-the-loop testbed for multi-agent-systems in a discrete event simulation: Integration of the Java agent development framework into plant simulation," in *Proc. IEEE Int. Syst. Eng. Symp. (ISSE)*, Oct. 2017, pp. 1–6.
[44] F. Jaensch, A. Csiszar, J. Sarbandi, and A. Verl, "Reinforcement learning of a robot cell control logic using a software-in-the-loop simulation as environment," in *Proc. 2nd Int. Conf. Artif. Intell. Industries (AI I)*, Sep. 2019, pp. 79–84.
[45] *Siemens Products Website*. Accessed: Jan. 15, 2022. [Online]. Available: https://new.siemens.com/it/it/prodotti/software.html

Graziana Cavone (Member, IEEE) received the master's degree *(summa cum laude)* in control engineering from the Polytechnic of Bari, Italy, in 2013, and the Ph.D. degree (Hons.) in electronic and computer engineering from the University of Cagliari, Italy, in 2018.

She has been a Research Fellow with the Polytechnic of Bari, Italy, where she currently is a Post-Doctoral Research Fellow, and a Visiting Ph.D. Student with the Delft University of Technology, The Netherlands, from 2016 to 2017. She is the author of more than 30 printed international publications. Her research interests include definition, simulation, and application of decision and control techniques to discrete-event and hybrid systems, manufacturing systems, logistics, energy systems, and smart cities. She was the Local Arrangements Chair of the 2021 Mediterranean Conference on Control and Automation. She was a member of the International Program Committee of more than 20 international conferences and a Guest Editor for Special Issues on international journals. She was awarded a research grant by the National Science Foundation of China for the year 2020. She is an Associate Editor of the international journal *Results in Control and Optimization* (RICO).

Augusto Bozza (Graduate Student Member, IEEE) received the bachelor's degree in computer science and automation engineering and the master's degree (Hons.) in automation engineering (with a specialization in robotics) from the Politecnico di Bari, Italy, in 2018 and 2021, respectively. His thesis was in "Design and test of real-time control systems for the cold metal sheet forming process in the automotive sector." He is currently pursuing the Ph.D. degree in electrical and information engineering with the Polytechnic University of Bari.

He is also working with the Decision and Control Laboratory, Department of Electrical and Information Engineering, Polytechnic University of Bari, where he was a Research Assistant in 2021. His research interests include modeling, control, and simulation of manufacturing and industrial systems.

Raffaele Carli (Senior Member, IEEE) received the Laurea degree (Hons.) in electronic engineering and the Ph.D. degree in electrical and information engineering from the Politecnico di Bari, Italy, in 2002 and 2016, respectively.

From 2003 to 2004, he was a Reserve Officer with Italian Navy. From 2004 to 2012, he worked as a System and Control Engineer and a Technical Manager for a space and defense multinational company. He is currently an Assistant Professor in Automatic Control with the Politecnico di Bari. He is the author of more than 60 printed international publications. His research interests include the formalization, simulation, and implementation of decision and control systems, as well as modeling and optimization of complex systems. He was a member of the International Program Committee for more than 20 international conferences and a guest editor for special issues on international journals.

Mariagrazia Dotoli (Senior Member, IEEE) received the Laurea degree (Hons.) in electronic engineering and the Ph.D. degree in electrical engineering from the Politecnico di Bari, Italy, in 1995 and 1999, respectively.

She has been a Visiting Scholar with Paris 6 University and the Technical University of Denmark. She is currently a Full Professor in Automatic Control with the Politecnico di Bari, which she joined in 1999. She has been the Vice Rector for research of the Politecnico di Bari and a member elect of the Academic Senate. She is the author of more than 200 publications, including one textbook (in Italian) and over 70 international journal articles. Her research interests include modeling, identification, management, control and diagnosis of discrete event systems, manufacturing systems, logistics systems, traffic networks, smart grids, and networked systems.

Prof. Dotoli is an Expert Evaluator of the European Commission since the 6th Framework Programme. She was a member of the International Program Committee of over 80 international conferences. She was the Co-Chairperson of the Training and Education Committee of ERUDIT, the European Commission network of excellence for fuzzy logic and uncertainty modeling in information technology, and was a Key Node Representative of EUNITE, the EUropean Network of Excellence on Intelligent Technologies. She is the General Chair of the 2021 Mediterranean Conference on Control and Automation. She was the Program Chair of the 2020 IEEE Conference on Automation Science and Engineering, the Program Co-Chair of the 2017 IEEE Conference on Automation Science and Engineering, the Workshop and Tutorial Chair of the 2015 IEEE Conference on Automation Science and Engineering, the Special Session Co-Chair of the 2013 IEEE Conference on Emerging Technology and Factory Automation, and the Chair of the National Committee of the 2009 IFAC Workshop on Dependable Control of Discrete Systems. She is a Senior Editor of the IEEE TRANSACTIONS ON AUTOMATION SCIENCE AND ENGINEERING and an Associate Editor of the IEEE TRANSACTIONS ON SYSTEMS, MAN, AND CYBERNETICS: SYSTEMS and the IEEE TRANSACTIONS ON CONTROL SYSTEMS TECHNOLOGY

Open Access funding provided by 'Politecnico di Bari' within the CRUI CARE Agreement